

Applied Meteorology Unit (AMU)
Quarterly Report
Fourth Quarter FY-98

Contract NAS10-96018

31 October 1998

ENSCO, Inc.
1980 N. Atlantic Ave., Suite 230
Cocoa Beach, FL 32931
(407) 853-8105 (AMU)
(407) 783-9735

Distribution:

NASA HQ/Q/F. Gregory
NASA HQ/AS/F. Cordova
NASA KSC/PH/R. Sieck
NASA KSC/PH/D. King
NASA KSC/PH/R. Roe
NASA KSC/AA-C/L. Shriver
NASA KSC/AA/R. Bridges
NASA KSC/MK/D. McMonagle
NASA KSC/PH-B/J. Oertel
NASA KSC/PH-B3/T. Greer
NASA KSC/AA-C-1/J. Madura
NASA KSC/AA-C-1/F. Merceret
NASA KSC/BL/J. Zysko
NASA KSC/DE-TPO/K. Riley
NASA JSC/MA/T. Holloway
NASA JSC/ZS8/F. Brody
NASA JSC/MS4/W. Ordway
NASA JSC/MS4/R. Adams
NASA JSC/DA8/W.Hale
NASA MSFC/EL23/D. Johnson
NASA MSFC/SA0-1/A. McCool
NASA MSFC/EL23/S. Pearson
45 WS/CC/D. Urbanski
45 WS/DOR/W. Tasso
45 WS/SY/D. Harms
45 WS/SYA/B. Boyd
45 RANS/CC/S. Liburdi
45 OG/CC/P. Benjamin
45 MXS/CC/J. Hanigan
45 LG/LGQ/R. Fore
CSR 1300/M. Maier
CSR 4140/H. Herring
45 SW/SESL/D. Berlinrut
SMC/CWP/D. Carroll
SMC/CWP/J. Rodgers
SMC/CWP/T. Knox
SMC/CWP/R. Bailey
SMC/CWP (PRC)/P. Conant
Hq AFSPC/DDOR/G. Wittman
Hq AFSPC/DORW/S. Carr
Hq AFMC/DOW/P. Yavosky
Hq AFWA/CC/J. Hayes
Hq AFWA/DNXT/R. Lefevre
Hq AFWA/DN/Freeman
Hq USAF/XOW/F. Lewis
Hq AFRL/XPPR/B. Bauman
Office of the Federal Coordinator for Meteorological Services and Supporting Research
SMC/SDEW/B. Hickel
SMC/MEEV/G. Sandall
NOAA "W/OM"/L. Uccellini
NOAA/OAR/SSMC-I/J. Golden
NOAA/ARL/J. McQueen
NOAA Office of Military Affairs/T. Adang

NWS Melbourne/B. Hagemeyer
NWS Southern Region HQ/"W/SR"/X. Proenza
NWS Southern Region HQ/"W/SR3"/D. Smith
NSSL/D. Forsyth
NWS/"W/OSD5"/B. Saffle
PSU Department of Meteorology/G. Forbes
FSU Department of Meteorology/P. Ray
NCAR/J. Wilson
NCAR/Y. H. Kuo
30 WS/CC/C. Davenport
30 WS/DOS/S. Sambol
30 SW/XP/R. Miller
NOAA/ERL/FSL/J. McGinley
SMC/CLNER/B. Kempf
Aerospace Corp./B. Lundblad
Tetrattech/NUS Corp./H. Firstenberg
ENSCO ARS Div. V.P./J. Pitkethly
ENSCO Contracts/M. Penn

Executive Summary

This report summarizes AMU activities for the fourth quarter of FY 98 (July - September 1998). A detailed project schedule is included in the Appendix.

Effective 31 July, Mr. Paul Nutter resigned his position with ENSCO and the AMU to pursue a Ph.D. in meteorology at the University of Oklahoma. Mr. Jonathan Case has been hired to fill his position in the AMU. Mr. Case recently earned his M.S. in meteorology from the University of Oklahoma.

Based on recommendations from SMG, Dr. Manobianco and Mr. Case participated in a teletraining session on hurricane models conducted at NWS MLB on 10 September. They found the teletraining to be effective. The AMU will consider teletraining in the future when appropriate to present results from AMU tasks.

Ms. Lambert consulted with the SMG, 45 WS, and NWS MLB to develop a work plan for the Statistical Short-Range Forecast Tools task. Several teleconferences were held to determine the weather elements for which forecasts would be developed. The elements chosen are listed in this report. After the elements were determined, Ms. Lambert began procedures to collect the necessary data from the appropriate agencies.

Several AMU personnel participated in RSA meetings and teleconferences. Mr. Wheeler participated in a teleconference discussing the RSA weather display systems for both ranges and Dr Taylor addressed a question from RSA about radar coverage over CCAS/KSC. Drs. Taylor and Manobianco, and Mr. Wheeler attended a meeting to discuss and clarify AMU data, communication bandwidth, and display requirements. Dr. Manobianco, Mr. Case, and Mr. Evans participated in a teleconference that addressed questions on the proposed analysis and modeling configuration designed to support toxics for RSA.

Mr. Wheeler continues to work with Mr. Weems (of the RWO) and CSR on the MIDDS/MIDDS-X transition by providing technical support in migrating the current functionality to the MIDDS-X weather display system. Approximately 75 different commands and/or output displays were tested or evaluated. In addition to discussions, feedback and shortfalls were provided to Mr. Weems and the CSR programmers.

Mr. Evans has completed the Delta Explosion Analysis project and is currently compiling the final report. Figures are shown in this report to demonstrate the results of a comparison between two numerical weather prediction models and the NWS MLB WSR-88D radar observations of the plume. The results indicate a good agreement between the models and the observations.

During the past quarter, Dr. Manobianco and Mr. Case modified the Local Data Integration System (LDIS) configuration to increase the number of passes in the objective analysis scheme used in the Advanced Regional Prediction System (ARPS) Data Analysis System (ADAS). In this quarterly report, the modified configuration of ADAS is discussed followed by a description of the Complex Cloud Scheme (CCS) used in ADAS. Results from two case examples demonstrate that the structure of the cloud analyses resembles the patterns in the reflectivity cross sections. The primary advantage of the CCS is that it integrates surface cloud, radar, and satellite observations to produce a more complete picture of cloud features over east central Florida. The capability to overlay analyzed cloud variables and other parameters such as temperature can also help forecasters to diagnose cloud properties and possible cloud electrification.

Dr. Merceret continued a study to determine the actual effective vertical resolution of the KSC 50-MHz Doppler Radar Wind Profiler (DRWP). He determined that the DRWP is usually Nyquist limited at 300 m. In collaboration with Dr. Stan Adelfang at NASA/MSFC, Dr. Merceret developed statistical analyses of high temperature extremes at the Shuttle launch complexes (LC-39 A, B) to assist the Shuttle program in deciding whether to modify its high temperature Launch Commit Criterion (LCC). Based on the results of the analyses, the program elected to retain the current LCC.

SPECIAL NOTICE TO READERS

AMU Quarterly Reports are now published on the Wide World Web (WWW). The Universal Resource Locator for the AMU Home Page is:

<http://technology.ksc.nasa.gov/WWWaccess/AMU/home.html>

The AMU Home Page can also be accessed via links from the NASA KSC Internal Home Page alphabetical index. The AMU link is "CCAS Applied Meteorology Unit".

If anyone on the current distribution would like to be removed and instead rely on the WWW for information regarding the AMU's progress and accomplishments, please respond to Frank Merceret (407-867-2666, francis.merceret-1@ksc.nasa.gov) or Ann Yersavich (407-853-8203, anny@fl.ensco.com).

1. BACKGROUND

The AMU has been in operation since September 1991. The progress being made in each task is discussed in Section 2 with the primary AMU point of contact reflected on each task and/or subtask.

2. AMU ACCOMPLISHMENTS DURING THE PAST QUARTER

2.1 TASK 001 AMU OPERATIONS

AMU personnel supported two expendable launch vehicle (ELV) launches (Titan and Delta) during the quarter.

Effective 31 July, Mr. Paul Nutter resigned his position with ENSCO and the AMU to pursue a Ph.D. in meteorology at the University of Oklahoma. Mr. Jonathan Case has been hired to fill his position in the AMU. Mr. Case recently earned his M.S. in meteorology from the University of Oklahoma. His areas of expertise include diagnoses of interactions between mesoscale and synoptic scale phenomena. He also has experience and interest in weather forecasting, numerical weather prediction, and climatology.

AMU HARDWARE AND SOFTWARE MAINTENANCE

Several new updates to software packages were loaded onto different workstations during the past quarter.

As we discovered last quarter during the major operating system upgrade to the IBM RS/6000 UNIX workstations, IBM will no longer be supporting UNIX to UNIX copy (UUCP) protocol for electronic mail transfer in the next release of the AIX Operating System. As a result, the AMU has been evaluating various PC-based electronic mail server software packages.

AMU MIDDS-X CONVERSION

During this quarter the AMU MIDDS-X terminals were setup and began to collect data. Mr. Wheeler began and continues to migrate the different commands and functionality currently used in the AMU over to the MIDDS-X workstations.

2.2 TASK 002 TRAINING

SMG recently received two teletraining sessions covering hurricane models. Dr. Bernard Meiser provided the training from NWS Southern Region Headquarters. Mr. David Sharp also indicated that teletraining is used by NWS MLB as part of their overall training efforts. Teletraining is conducted remotely using PCs, modems, and appropriate software with audio provided by via conference phone. Several sites can be accommodated at once. As such, it is cost effective because instructors and students have two-way interactions during the fully electronic presentation without requiring travel expenses to bring them together in the same location.

SMG noted that teletraining is quite effective and suggested that it may be a good method to brief the status and results of AMU tasks. Based on these recommendations, Dr. Manobianco and Mr. Case participated in the training session on hurricane models conducted at NWS MLB on 10 September. They also found teletraining to be effective. The AMU will consider teletraining in the future when appropriate to present results from AMU tasks.

Mr. Wheeler provided startup and functionality training to the AMU personnel on the new MIDDs-X weather display system. The Graphical User Interface (GUI) was reviewed in detail. Mr. Wheeler also described and demonstrated string tables, command line McBASi and batch file interaction.

2.2 TASK 003 SHORT-TERM FORECAST IMPROVEMENT

SUBTASK 3 STATISTICAL SHORT-RANGE FORECAST TOOLS (MS. LAMBERT)

During this quarter, Ms. Lambert developed a draft task plan that was electronically mailed to the customers at SMG, 45 WS, and NWS MLB. A teleconference was then held between the AMU and the customers in September to discuss how the task should be specifically defined. As a result of this teleconference, the customers were asked to provide lists of weather elements considered most important to their operations. These lists included the weather elements ranked according to importance as well as the spatial and temporal extent of the forecast desired.

Once the lists were received by the AMU, Ms. Lambert determined the data types that would be needed and the probability that a successful statistical forecast could be developed within one year for each of the elements. This information was distributed to the customers and another teleconference was held to determine which of the weather elements on the lists would become part of the task. The subsets of elements chosen for this task from each list are shown in Tables 1 to 3. After the elements were determined, Ms. Lambert began procedures to collect the necessary data from CSR, Air Force Combat Climatology Center (AFCCC), National Climatic Data Center (NCDC), and National Data Buoy Center (NDBC).

Table 1 Subset of weather elements suggested by the 45 WS that were chosen for the task. Elements are in rank order.		
<i>Weather Element</i>	<i>Forecast Time Period</i>	<i>Forecast Location</i>
1. Non-convective winds at launch pads Specific requirements vary with vehicle/payload	0-8 hrs, every hour (mainly cool season)	Launch pad towers
2. Other non-convective wind (V) forecasts: CCAS (sfc - 200 ft): $35 \leq V < 50$ kt $V \geq 50$ kt Port (sfc - 54 ft): $V \geq 22$ kt KSC (sfc - 300 ft): $35 \leq V < 50$ kt $50 \leq V < 60$ kt $V \geq 60$ kt	Lead time 30 min Lead time 60 min Lead time 30 min Lead time 30 min Lead time 60 min Lead time 60 min	CCAS tower network Port tower network KSC tower network

Table 2 Subset of weather elements suggested by the SMG that were chosen for the task. Elements are in rank order.		
<i>Weather Element</i>	<i>Forecast Time Period</i>	<i>Forecast Location</i>
1. Clouds a) Ceilings (actual reported value) b) Amounts (clr, sct, bkn, ovc) c) Base heights (reported value)	0-8 hrs, every hour (mainly cool season)	SLF surface observation
2. Wind speed and direction a) Peak wind speed b) 2-min average wind speed c) 2-min average wind direction	0-6 hrs, every 1/2 hour 0-6 hrs, every 1/2 hour 0-6 hrs, every 1/2 hour	Tower 313, SLF towers
3. Visibility	0-6 hrs, every hour	SLF surface observation

Table 3 Subset of weather elements suggested by the NWS MLB that were chosen for the task. Elements are in rank order.		
<i>Weather Element</i>	<i>Forecast Time Period</i>	<i>Forecast Location</i>
1. Clouds Amounts and base heights Ceiling values for LIFR, IFR, MVFR, and VFR	0-6 hrs, every hour	MLB, MCO, DAB, VRB
2. Visibility Values for LIFR, IFR, MVFR, and VFR	0-6 hrs, every hour	MLB, MCO, DAB, VRB
3. Wind speed/direction	0-6 hrs, every hour	MLB, MCO, DAB, VRB

2.3 TASK 004 INSTRUMENTATION AND MEASUREMENT

SUBTASK 5 I&M AND RSA SUPPORT (DR. MANOBIANCO/MR. WHEELER)

During July, Mr. Wheeler participated in a teleconference discussing the RSA weather display systems for the Eastern and Western Ranges. It was decided that prior to the RSA changes, the Eastern Range would continue the migration to MIDDs-X and the Western Range would continue to use WFO-Advanced.

During August, Dr Taylor addressed a question from RSA about radar coverage over CCAS/KSC. He calculated the bottom, middle point, and top of the lowest elevation scans of the Melbourne WSR-88D and the Patrick AFB WSR-74C radars at the distance from each radar to Launch Complex 39A. The results from these calculations were provided to Mr. Billie Boyd (45 WS) and Major Scot Heckman (USAF Space Command).

Drs. Taylor and Manobianco, and Mr. Wheeler attended a meeting with representatives from Lockheed-Martin Raytheon (LMR) to discuss and clarify AMU data, communication bandwidth, and display requirements. LMR will use the information from this meeting to develop their approach and cost estimates for including the AMU within the Spacelift Range System.

Dr. Manobianco, Mr. Case, and Mr. Evans participated in a teleconference with representatives from the USAF Space Command, Eastern and Western Range weather and safety, NASA KSC Weather Office, and Forecast Systems Laboratory (FSL). The purpose of this teleconference was to have FSL personnel provide an overview and address questions, issues, and concerns on the proposed analysis (LAPS) and modeling (RAMS) configuration designed to support toxics for RSA.

SUBTASK 9 MIDDS-X TRANSITION (MR. WHEELER)

Mr. Wheeler continues to work with the Mr. Weems (45 WS/RWO) and CSR on the MIDDS/MIDDS-X transition by providing technical support in migrating the current functionality to the MIDDS-X weather display system. Approximately 75 different commands and/or output displays were tested or evaluated. In addition to discussions, feedback and shortfalls were provided to Mr. Weems and the CSR programmers.

2.4 TASK 005 MESOSCALE MODELING**SUBTASK 4 DELTA EXPLOSION ANALYSIS (MR. EVANS)**

The Delta Explosion Analysis project is being funded by KSC under AMU option hours. The primary goal of this task is to conduct a case study of the explosion plume using the RAMS, REEDM, and HYPACT models and compare the model results with available meteorological and plume observations. The Melbourne WSR-88D radar data was analyzed and provided information on the location and track of the clouds following the explosion. The location of the predicted plume was determined by analyzing the HYPACT output showing the location of the plume particles for 10-minute periods from 1630 UTC until 2030 UTC.

The analysis has been completed and the results are being included into the final report. The compilation of the draft final report is ongoing and should be completed in early November.

There were two reasons for the modeling exercise of comparing the observed and predicted plumes. The principal of the two reasons was to determine how well the modeled plume trajectories compared with the observed plume trajectories. The secondary reason for the exercise was to determine how the REEDM-predicted source term compared with the actual source term. To reduce the amount of runs and the amount of figures we displayed, we combined the trajectory and source term analysis in the ERDAS-HYPACT runs and we did not perform a source term analysis for the PROWESS-HYPACT runs. Combining the runs did not hinder the results since we adequately assessed the trajectories of both runs and we were able to assess how the REEDM-predicted source term compared with the actual source term.

The figures presented in this report compare the predicted plume locations from ERDAS-HYPACT and PROWESS-HYPACT with the observed plume locations from the WSR-88D radar. The comparisons presented are for three different times during the four hours that the plume was tracked. The HYPACT source terms were generated from the REEDM model using the REEDM function of ERDAS. REEDM generates the HYPACT source term for a rocket launch by creating a column that contains mass of the chemical species of interest. The column is composed of separate sources (volumes) of mass, which are 75 meters in thickness. We assessed the REEDM-predicted source term by observing how the modeled initial plume changed during the simulation and comparing its shape with observed plume. The ERDAS-HYPACT run was made leaving the mass in the entire column from the surface up to 2500 meters. We assessed the ERDAS-HYPACT trajectories by tracking only the lower and upper part of the plume and comparing those with the trajectory of the observed plume.

The source term for the PROWESS configuration was modified slightly to simulate the observed source term since in our analysis we knew the initial shape of the plume. The plume was modified by removing the initial mass in the layers between 925 and 1550 meters. We assessed the PROWESS-HYPACT trajectories by tracking the two plumes and comparing those with the observed plume.

Figures 1 to 3 show the predicted and observed plumes at 1700 UTC and Figures 4 to 6 show the predicted and observed plumes at 1830 UTC. For the explosion time, both ERDAS-HYPACT and PROWESS-HYPACT transported the upper and lower explosion clouds in different directions. The split transport occurred because the upper cloud was at a height where the winds were strong and from the west while the lower cloud was trapped below a strong inversion where winds were from the north.

The primary purpose of analyzing the trajectory of the ERDAS-HYPACT and PROWESS-HYPACT plumes was to determine how the model predictions compared with observations. Therefore, the discussion below focuses on comparisons of the lower plume below 925 meters and the upper plume above 1550 meters. Even though the

ERDAS-HYPACT simulation was run with the entire plume, we were not concerned with the transport of the center of the plume between 925 and 1550 meters.

HYPACT moved the lower cloud to the south where it reached the coast in the vicinity of Cocoa Beach at approximately 30 minutes after the explosion. Figure 1 shows the lowest part of the ERDAS cloud out over the ocean and extending westward to the coastline where it curves north and then east. Figure 2 shows the two PROWESS clouds due to the initial source split with the lower cloud to the southwest of the upper cloud. The lower cloud extends upward and westward from over the ocean to the coastline. The upper cloud extends eastward and upward from approximately 10 km offshore out to approximately 20 km offshore.

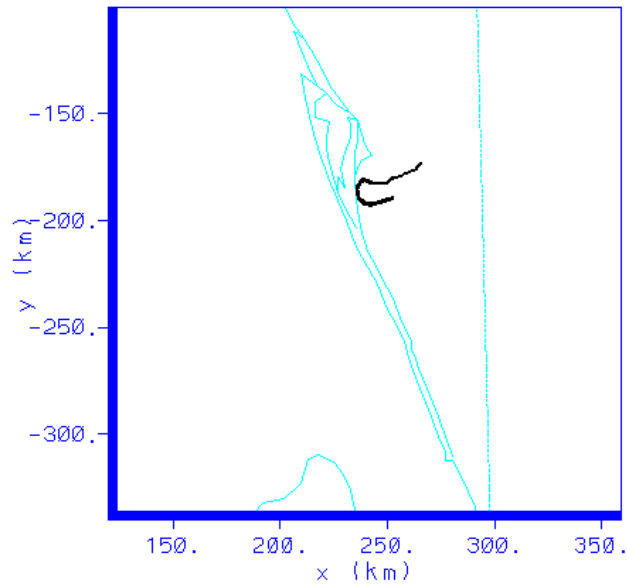
The observed radar plume at 1700 UTC shows that the low-level cloud had reached the coast north of Cocoa Beach and had moved slightly more westward than the model runs had predicted (Fig. 3). The orientation of the cloud was east-west in a shape similar to the model predictions. The upper cloud was also oriented in an east-west direction as it was transported eastward by the westerlies.

At 1830 UTC approximately two hours after the explosion, the ERDAS and PROWESS HYPACT runs moved the low-level cloud to the south and spread it wider to the east and west (Figs. 4 and 5). The ERDAS low-level cloud extended slightly further west than the PROWESS low-level cloud. The upper cloud continued to move quickly to the east in both runs.

The observed radar plume at 1830 UTC consisted of two distinct clouds. The low-level cloud was located over Melbourne with part of the cloud extending eastward over the ocean. The bulk of the cloud was located over the land, to the west of where the model runs had predicted. The observed upper cloud matched the model predictions closely in its orientation from east-northeast to west-southwest and in its movement toward the east-southeast.

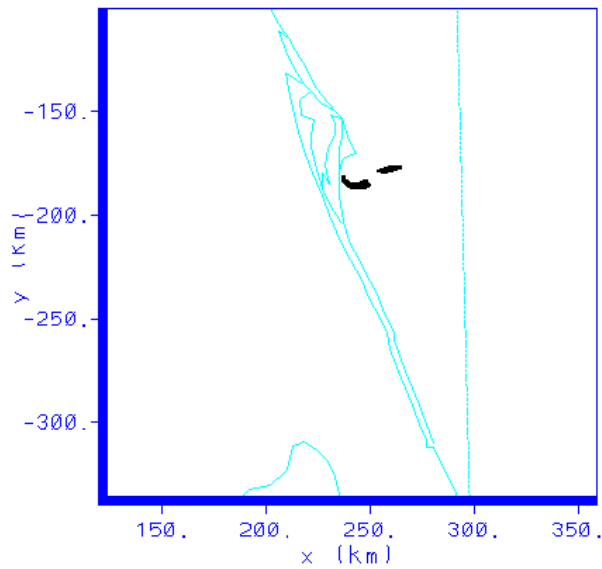
The discussion that is provided in this quarterly report indicates that the RAMS/HYPACT predictions of the lower cloud's direction of movement, speed, and dispersion matched closely with observations. However, the onshore component of the winds affecting the observed plume appeared stronger than the RAMS modeled winds. This was indicated by the observed plume moving more to the west than the modeled plume. The model's prediction of the upper cloud's direction and shape showed good agreement with the observed plume's direction and shape.

The source term used for the PROWESS-HYPACT (split column source term) run was a better fit than the source term used for ERDAS-HYPACT (continuous column source term). This result is not surprising since we decided to use the split column after viewing video and photography of the explosion cloud. The continuous column source term, however, showed a separation of the upper and lower clouds which began to take place at approximately 1830 UTC at a height of about 1100 meters. The separation was due to the strong shear above and below the strong inversion that existed and that was predicted by RAMS.



z = 187.5 m 1700 UTC

Figure 1. ERDAS-HYPACT plume at 1700 UTC on 17 January 1997. The lowest part of the cloud (surface) is at the tip of the “hook” while the highest part (2500 meters) is the point to the northeast. LC-17 is located just southwest of the tip of Cape Canaveral.



z = 187.5 m 1700 UTC

Figure 2. PROWESS-HYPACT plume at 1700 UTC on 17 January 1997. The lowest part of the cloud (surface) is at the eastern end of the cloud located to the southeast while the highest part (2000 meters) is at the eastern end of the cloud located to the northeast. LC-17 is located just southwest of the tip of Cape

Canaveral.

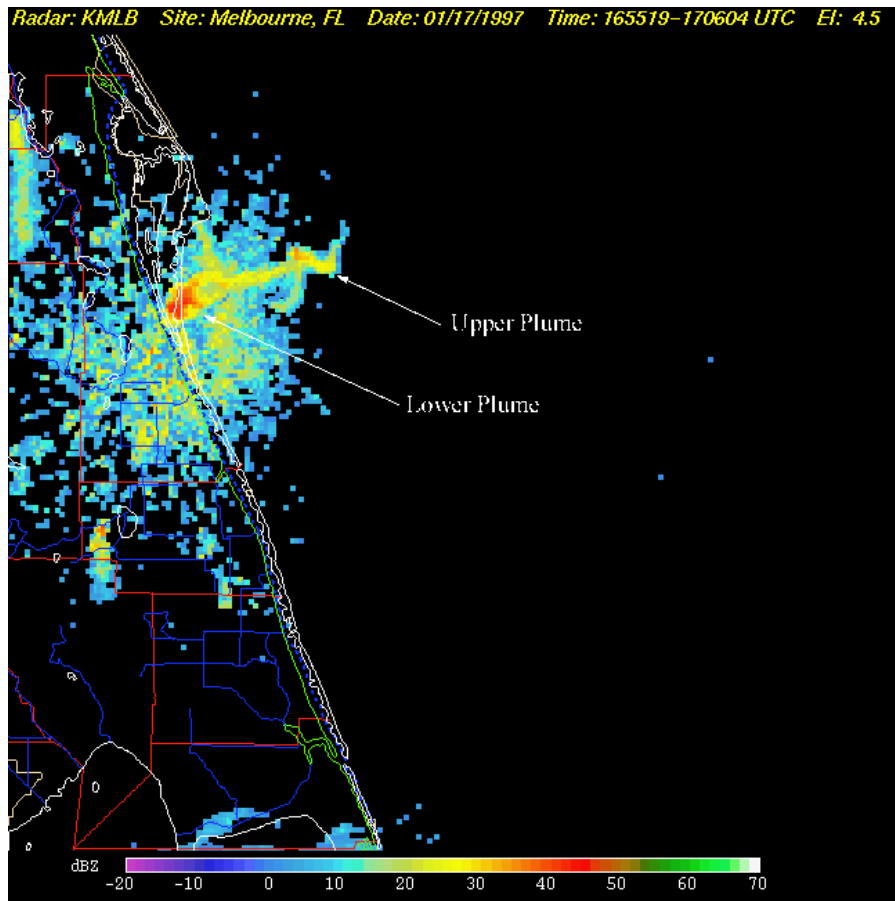
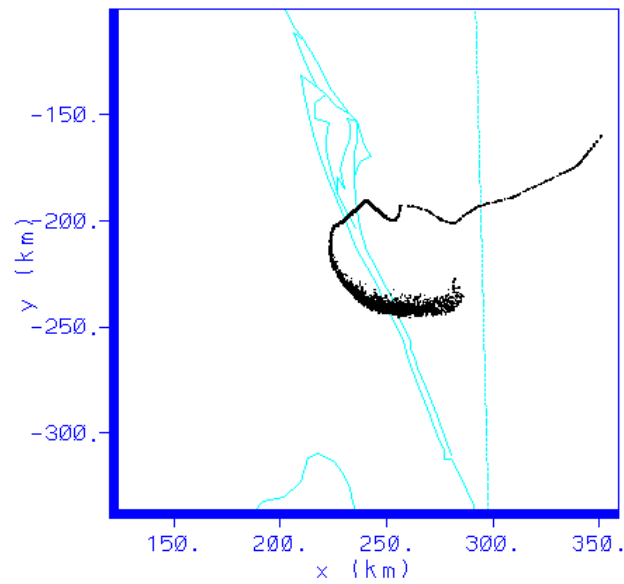
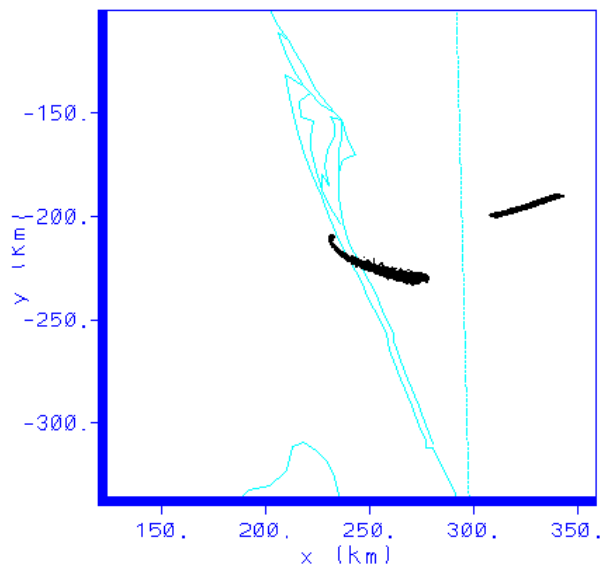


Figure 3. WSR-88D image at approximately 1700 UTC on 17 January 1997 showing the location of the observed cloud. The lower cloud is indicated by the large area of red reflectivities located northeast of Melbourne. The small area of red reflectivities located to the east over the ocean indicates the upper cloud.



z = 187.5 m 1830 UTC

Figure 4. ERDAS-HYPACT plume at 1830 UTC on 17 January 1997. The lowest part of the cloud (surface) is at the tip of the “hook” while the highest part (2500 meters) is the point to the northeast. LC-17 is located just southwest of the tip of Cape Canaveral.



z = 187.5 m 1830 UTC

Figure 5. PROWESS-HYPACT plume at 1830 UTC on 17 January 1997. The lowest part of the cloud (surface) is at the eastern end of the cloud located to the southeast while the highest part (1900 meters) is at the eastern end of the cloud located to the northeast. LC-17 is located just southwest of the tip of Cape

Canaveral.

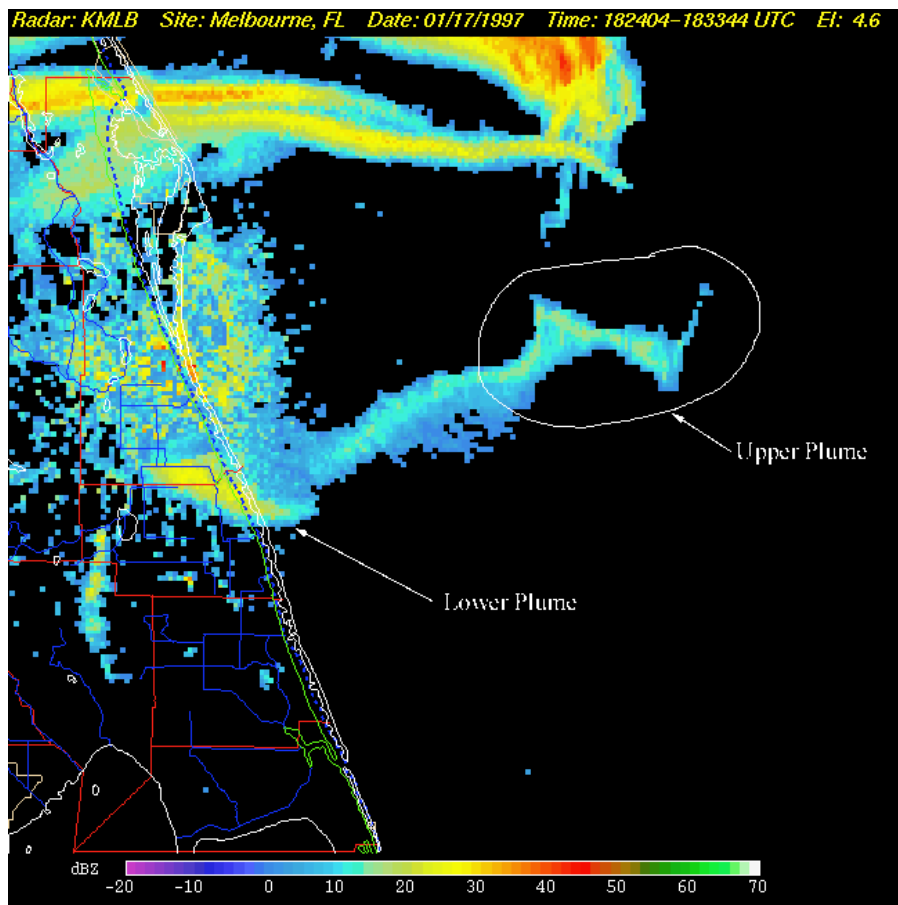


Figure 6. WSR-88D image at approximately 1700 UTC on 17 January 1997 showing the location of the observed cloud. The large area of yellow reflectivities located in southern Brevard County indicates the lower cloud. The small area of blue and yellow reflectivities located to the east over the ocean indicates the upper cloud. The large area of ribbon-like radar echoes stretching from west to east in the area north of Cape Canaveral are anomalous returns and do not indicate smoke or precipitation particles.

SUBTASK 5 MODEL VALIDATION PROGRAM (MR. EVANS)

The primary purpose of the U.S. Air Force's Model Validation Program (MVP) Data Analysis project, which is being funded by option hours from the U.S. Air Force, is to produce RAMS and HYPACT data for the three MVP sessions conducted at Cape Canaveral in 1995-1996. This program involves evaluation of Range Safety's modeling capability using controlled releases of tracers from both ground and aerial sources.

The status of the MVP data analysis tasks is presented in Table 4.

MVP Data Analysis Task	Session I	Session II	Session III
Prepare Data	Completed	Completed	Completed
Run ERDAS-RAMS	Completed	Completed	Completed
Run ERDAS-HYPACT	Completed	Completed	Completed
Run PROWESS-RAMS	Completed	Partially completed	Completed
Run PROWESS-HYPACT	Completed	Completed	Completed
Submit Data to NOAA-ATDD	Completed	To be done	Completed

The analysis of the MVP data for the three sessions is almost complete. RAMS data has been produced for the days of all releases and HYPACT runs are being finalized. Session II RAMS data was produced using 2.5-degree NCAR reanalysis data for initialization. Session III ERDAS-HYPACT runs were rerun due to a software bug that caused an error in the ERDAS concentrations but not the PROWESS concentrations.

SUBTASK 6 EXTEND 29-KM ETA MODEL OBJECTIVE EVALUATION (DR. MANOBIANCO)

During July, Mr. Nutter completed revisions to the final report entitled “*An Extended Objective Evaluation of the 29-km Eta Model for Weather Support to the United States Space Program*”. The back cover of the report includes a removable booklet and HTML formatted diskette designed to summarize results for operational forecast applications. Additional copies of the report, operations summary booklet and diskette are available and can be obtained by contacting Dr. Manobianco (johnm@fl.ensco.com).

In March 1998, Dr. Manobianco and Mr. Nutter submitted two manuscripts to the editors of *Weather and Forecasting*. These papers describe selected results from the subjective and objective portions of the meso-eta model evaluation. The manuscripts were accepted for publication and will appear in the June 1999 issue of *Weather and Forecasting*.

SUBTASK 7 LOCAL DATA INTEGRATION SYSTEM / CENTRAL FLORIDA DATA DEFICIENCY (DR. MANOBIANCO)

Beginning with the July 1998 AMU monthly activities report, the first part of the title for subtask 7 was changed from Data Assimilation Model to Local Data Assimilation System (LDIS). Although the Data Assimilation Model was referenced in previous reports as the LDIS, the new title makes it clear that subtask 9 under AMU Mesoscale Modeling Task 5 is an extension of this task.

During the past quarter, Dr. Manobianco and Mr. Case modified the LDIS configuration to increase the number of passes in the Bratseth objective analysis scheme (Bratseth 1986) as used in the Advanced Regional Prediction System (ARPS) Data Analysis System (ADAS; Brewster 1996; Carr et al. 1996). A data non-incorporation (DNI) test using ADAS was proposed and implemented by Dr. Manobianco and Mr. Case. The DNI effort is designed to assess the impact that specific data sources have on the subsequent analyses for the warm and cool season cases. Dr. Manobianco analyzed results from the DNI experiments by computing spatial correlation coefficients (CCs) between the full analysis and each DNI run. Spatial CCs measure the degree to which patterns are similar between two fields. Therefore, CCs near 0 (1) indicate that the data sources have relatively more (less) impact on the resulting analyses.

In this quarterly report, the modified configuration of ADAS is discussed followed by a description of the Complex Cloud Scheme (CCS) used in ADAS (Zhang et al. 1998). A previous AMU quarterly report (First Quarter FY-98) presented 2-km ADAS wind analyses of an outflow boundary in the warm season case. Therefore, results presented here will focus on the utility of the CCS and its cloud products. The influences of radar data and METAR cloud observations on the cloud analysis products are also discussed.

LDIS Configuration

The configuration of ADAS follows the layout used for the terminal wind analysis in the Integrated Terminal

Weather System (ITWS; Cole and Wilson 1995). ADAS is run every 15 minutes at 0, 15, 30, and 45 minutes past the hour, over an outer and inner grid with horizontal resolutions of 10 km and 2 km, respectively. The 10-km (2-km) analysis domain covers an area of 500×500 km (200×200 km), and consists of 30 vertical levels that extend from the surface to about 16.5 km above ground level. The vertical levels are stretched with the finest resolution near the surface (20 m spacing) and the coarsest resolution at upper levels (~1.8 km spacing).

The background fields used on the 10-km analysis domain are the Rapid Update Cycle (RUC; Benjamin et al. 1998) grids of temperature, wind, relative humidity, and height at 25-mb intervals from 1000 to 100 mb. The RUC analyses are available at a horizontal resolution of 60-km (40-km) every 3-h (1-h) for a warm (cool) season case (as discussed later in this subsection). The RUC grids are linearly interpolated in time every 15 minutes for each 10-km ADAS cycle. The resulting 10-km analysis grids are then used as background fields for analyses on the 2-km domain. This nested-grid configuration and cascade-of-scales analysis follows that used for terminal winds in ITWS. With such an approach, it is possible to analyze for different temporal and spatial scales of weather phenomena.

The wide variety of observational data used in the LDIS provides measurements at many different times. The version of ADAS used for the LDIS described here is configured to ingest data closest to the analysis time within a 15-minute window (± 7.5 minutes) centered on the analysis time. This data incorporation strategy is designed to simulate an operational configuration that would start each cycle after the actual analysis time to allow for the transmission, receipt and processing of real-time data.

Since the analysis cycle is run every 15 minutes over very fine scales, it is also necessary to ingest some data using non-standard methods. For synoptic-scale analyses, rawinsondes are assumed to provide vertical profiles of moisture, temperature, and winds at a single time and location. However, the balloon can drift a significant distance from the launch site during ascent depending on the speed and direction of the environmental wind. Furthermore, balloons used for upper air measurements ascend at a rate of about 5 m s^{-1} so observations are collected over a period of about one hour. To account for balloon drift, the rawinsonde measurements ingested by ADAS are treated as single-level observations each with an appropriate horizontal and vertical location that is determined using the ascent rate and observed winds. These single-level rawinsonde observations are then grouped into 15-minute bins centered on each analysis time. As a result, only a segment of the rawinsonde profile is used for each analysis cycle.

The KSC/CCAS tower data also require a specific strategy to ingest observations into ADAS. Many of the towers provide measurements at multiple levels ranging from 1.8 to 150 m. In order to incorporate tower data in ADAS, multi-level measurements from each tower are treated as soundings. In this way, data from the same tower at multiple levels can be used in the analysis based on fixed observation heights.

The observational data are incorporated into ADAS using multiple passes of the Bratseth scheme to account for the varying spatial resolution of the data sources. Five computational passes are used for the 10-km grid and four passes are utilized on the 2-km grid. Data with similar resolutions are grouped together in the same computational pass such that ADAS incorporates each data source without excessively smoothing the resolvable meteorological features. This methodology ensures that each data source is utilized in ADAS to its maximum potential based on the meteorological features that the data can resolve.

Complex Cloud Scheme of ADAS

The Complex Cloud Scheme (CCS) serves as the basis for moisture data assimilation in the ARPS mesoscale model. The CCS is based on the Local Analysis and Prediction System (LAPS; McGinley 1995) but includes a number of improvements and modifications following Zhang et al. (1998). The CCS incorporates a variety of data and empirically derives a number of cloud and moisture products utilizing a Barnes objective analysis procedure. The Barnes rather than Bratseth scheme is used in the CCS because LAPS was originally developed using a Barnes scheme.

The data used by the CCS are METAR cloud observations, satellite infrared and visible imagery, and radar reflectivity. The products derived from these data include three-dimensional (3D) cloud cover, fractional cloud cover, cloud liquid water (q_c) and cloud ice water (q_i) mixing ratios, cloud and precipitate types, in-cloud vertical

velocity, icing severity index, rain/snow/hail (q_r , q_s , q_h) mixing ratios, cloud base, cloud top, and cloud ceiling fields. Furthermore, the CCS enhances the specific humidity (q_v) within areas of analyzed clouds.

The analyzed cloud fields are generated by combining available METAR, radar, and satellite data. METAR and infrared satellite data provide information about the bottom and top of the cloud decks, respectively, whereas radar data fill in the gaps to create a vertically continuous cloud field. Data are linearly interpolated between successive radar beams to provide continuity in the derived cloud fields. Albedo data derived from the visible imagery are primarily used for the removal of excess cloud cover in the analysis (Zhang et al. 1998; Albers et al. 1996).

No data source used in the CCS can provide an actual measurement of cloud thickness. Since there is no information about the thickness of the clouds in the METAR reports, an empirically derived thickness of roughly 1 km is assigned in the CCS for each cloud layer reported (Albers et al. 1996). The advantage of using METAR observations is that they provide surface-based cloud observations. Therefore, cloud decks can be analyzed by the CCS when they can be not be observed by radar or satellite. For example, high clouds may obscure satellite observations of low clouds or low clouds may form below the lowest elevation angle of the radar beam. One current problem is that standard METAR observations are available once per hour. Since ADAS is run every 15 minutes, a discontinuity can occur in the cloud analysis due to the lack of METAR observations at off-hour times.

Brief Overview of the Two Case Studies

A series of control analyses was generated for both a warm (26-27 July 1997) and cool season (12 December 1997) case study in order to examine the fidelity and utility of ADAS wind and cloud parameters. These analyses serve as the basis for the discussion of each event in this report. The highlights and motivation for selecting each case are given below.

The Warm Season Event (26-27 July 1997)

A typical, undisturbed warm season environment characterized the 26-27 July 1997 case. Early in the afternoon, scattered thunderstorms developed across the peninsula and a sea-breeze boundary was evident along the east coast. Later in the afternoon, strong thunderstorms developed southwest of KSC/CCAS and generated an outflow boundary that propagated northeastward. This outflow boundary caused wind gusts greater than 15 m s^{-1} as noted on the KSC/CCAS mesonet towers around 2245 UTC. This case was chosen because the strong winds associated with the outflow boundary forced Atlas launch operation A1393 to be scrubbed for the day.

The Cool Season Event (12 December 1997)

The cool season case featured a slow moving cold front accompanied by widespread post-frontal precipitation with embedded thunderstorms. The structure of the wind shift line was detected well by the KSC/CCAS 915-MHz profiler data prior to the onset of precipitation. Northerly winds up to 10 m s^{-1} and widespread low cloud cover followed the frontal passage over the KSC/CCAS region. The Melbourne, FL WSR-88D indicated a well-defined reflectivity gradient along the leading edge of the front later on 12 December. This case was selected in order to assess the value of a LDIS during a weak frontal passage and widespread precipitation event across central Florida.

Cloud Analysis Results from the Case Studies

The CCS has the capability to provide forecasters valuable information about the properties of clouds. With suitable visualization and display techniques, fast and efficient assessments of the evolution of cloud structures can be conducted to help determine cloud thickness, cloud heights, ceilings, and the potential for cloud electrification and lightning. The results presented in this section illustrate the role of radar data in the CCS of ADAS for both the warm and cool season cases. In addition, the utility of the CCS is highlighted by focusing on its advantages over conventional reflectivity cross sections. Finally, the influence of METAR cloud reports is shown for the cool season case.

Impact of WSR-88D Reflectivity Data

WSR-88D reflectivity data are critical in the CCS since cloud parameters are empirically derived from

threshold values of reflectivity. Also, reflectivity data provide the most continuous source for generating the 3D structure of the cloud fields. A drawback of radar data is that each beam slopes upward with distance from the radar site. At significant distances from the radar location, the lowest elevation scan can overshoot areas of low cloud cover. This problem is partly alleviated by the incorporation of hourly METAR cloud reports that include information about the height of the cloud base.

The WSR-88D reflectivity data are compared to the cloud products from the 2-km ADAS analyses. Cross sections of reflectivity and cloud products are taken along the same lines areas in order to make these qualitative comparisons. An exact correspondence between the reflectivity and cloud images should not be expected since the CCS also uses METAR and satellite data to construct the 3D cloud fields.

For the warm season case of 26 July 1997, thunderstorms to the southwest of KSC/CCAS are examined in order to compare the analyzed cloud structure to the reflectivity images. A large cluster of reflectivity exceeding 34 dBZ lies over southern Brevard and eastern Osceola counties at 2212 UTC (Fig. 7a). Within this maximum of high reflectivity are embedded areas of reflectivity greater than 50 dBZ. The coverage and intensity of this reflectivity maximum decreases slightly by 2242 UTC as the widespread convection moves northeastward (Fig. 7b).

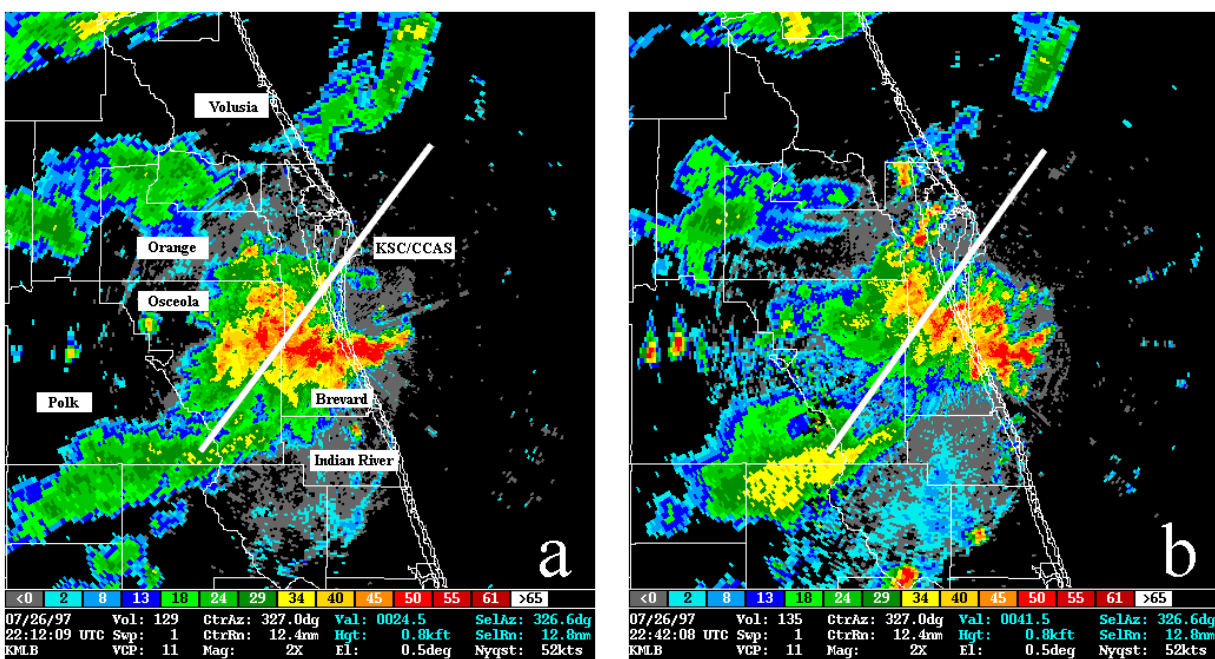


Figure 7. Base reflectivity images are shown from the Melbourne, FL WSR-88D on 26 July 1997 at (a) 2212 UTC and (b) 2242 UTC. Locations of counties and KSC/CCAS are denoted in panel a.

Southwest–northeast oriented cross sections through these thunderstorms along the lines in Figure 7 reveal the structure of the derived cloud variables from the 2-km ADAS analyses and allow for comparisons between radar reflectivity and the analyzed cloud fields. Note that the reflectivity and cloud cross sections shown in Figure 8 are along the exact same cross section line. The reflectivity cross section at 2212 UTC shows three distinct bands of heavy precipitation below 5 km (labeled with arrows 1, 2, and 3 in Fig. 8a). Reflectivity > 50 dBZ exists in columns associated with cells 1 and 2 whereas cell 3 has a weaker but still distinct reflectivity maxima. The corresponding 2-km ADAS cross section of cloud parameters (Fig. 8b) resembles the radar cross section qualitatively with a few minor variations. The best correspondence between Figures 8a and b occurs in the rain water (q_r) field. The most concentrated columns of q_r coincide with the regions of highest reflectivity as depicted by the cells 1, 2, and 3 in Figure 8b. A similar correspondence is evident between the reflectivity and q_r fields in Figures 8c and d especially with respect to the heaviest cell shown by the arrow.

The same series of radar and cloud analysis figures is displayed for the cool season case at 1700 UTC and 1900

UTC 12 December. The base reflectivity images are shown first followed by northwest–southeast cross sections of reflectivity and cloud variables. At 1700 UTC, a southwest–northeast elongated band of precipitation, with embedded areas of heavier convection, extends from northwestern Polk County through much of Volusia County (Fig. 9a). Isolated convection occurs ahead of this precipitation across the KSC/CCAS region. The main band of precipitation drifts southeastward over the next two hours and reaches the northern half of Brevard county by 1900 UTC (Fig. 9b). A line of heavy thunderstorms, positioned over northwestern Brevard, central Osceola, and southern Polk counties, marks the leading edge of the precipitation at this time.

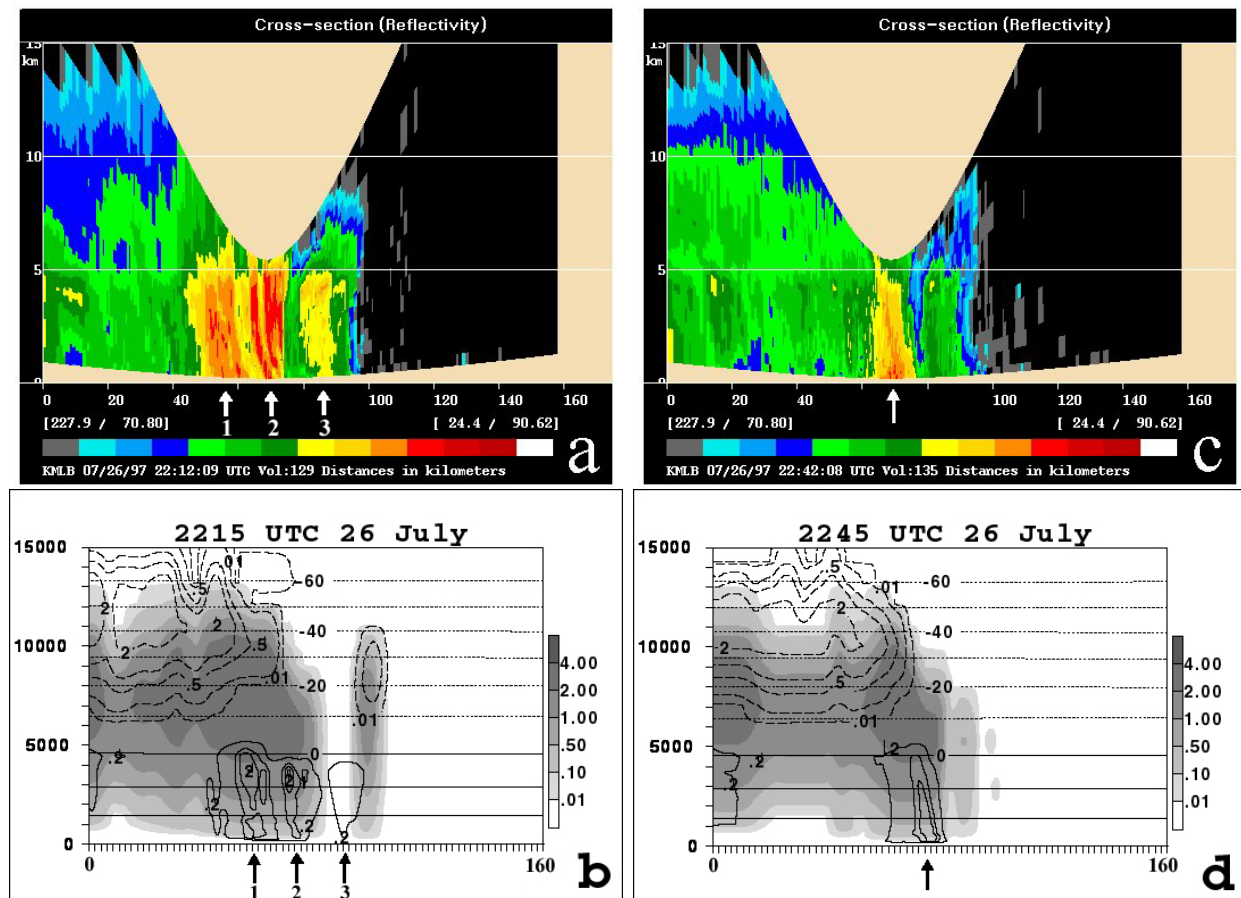


Figure 8. Cross sections of radar reflectivity from the Melbourne WSR-88D and 2-km ADAS analyses of cloud water mixing ratio (q_c), rain water mixing ratio (q_r), and cloud ice mixing ratio (q_i). All cross sections are taken along the lines shown in Figure 7. Reflectivity cross sections are shown at 2212 UTC and 2242 UTC 26 July 1997 in panels a and c, respectively, while analysis cross sections are shown at 2215 UTC and 2245 26 July 1997 in panels b and d, respectively. The vertical axes range from the surface to 15 km while the horizontal axes range from 0 to 160 km. The q_c fields (g kg^{-1}) are shaded according to the gray scale in panels b and d. The q_r (g kg^{-1}) and q_i (g kg^{-1}) fields are shown by the solid and dashed lines, respectively, in panels b and d. Note that isopleths for q_r (q_i) are given at 0.2, 1.0, 1.5, and 2.0 g kg^{-1} (0.01, 0.1, 0.5, 1.0, and 2.0 g kg^{-1}). Horizontal lines in panels b and d denote isotherms every 10 °C with negative temperatures shown by dotted lines. Individual cells are marked by arrows.

A northwest–southeast cross section through the area of precipitation at 1700 UTC reveals excellent correspondence between the radar cross section (Fig. 10a) and cloud products (Fig. 10b). The heaviest convective cell over KSC/CCAS at 1700 UTC (Fig. 10a) is depicted quite well in the cloud analysis cross section as noted by the concentrated column of cloud water (q_c) and q_r (arrow in Figure 10b). The uniform area of 18–29 dBZ reflectivity in the left portion of Figure 10a (at and below 7.5 km) is denoted by the 2-km ADAS q_c and cloud ice

(q_i) fields between 2.5 km and 7.5 km (Fig. 10b). Furthermore, somewhat of an ice anvil is seen between 9 km and 12 km with maximum q_i exceeding 1.0 g kg^{-1} . By 1900 UTC, the thickest and most concentrated q_c shifts southeastward (Fig. 10d), corresponding to the maximum reflectivity in Figure 10c. Again, the q_r field is in close agreement with the highest reflectivities as denoted by the embedded cells labeled with arrows 1 and 2 in Figures 10c and d.

It is interesting to note the substantial cone of silence above 5 km in the center of the warm season radar cross sections (Figs. 8a and c). The influence of the cone of silence is somewhat visible in the cloud analysis as noted by the downward sloped q_c fields above cells 1 and 2 (Fig. 8b). However, this data void is not as prevalent in the cloud analyses because the CCS interpolates data in three dimensions between radar beams and blends the data with the background. Furthermore, the incorporation of GOES-8 IR data builds cloud information at upper levels. These characteristics of the CCS lessen the impact of the cone of silence on the analyzed 3D cloud fields.

Another characteristic of radar data is the upward slope of the beams with distance from the radar site. The influence of the sloped radar beams on the cloud analysis is clearly depicted in Figure 8. The lower edge of the reflectivity data extends upward from the center to the endpoints of the cross section ($\sim 1.0\text{--}1.5 \text{ km}$ in Figs. 8a and c) which corresponds to the upward slope of the lowest elevation scan. This same pattern exists in the analyzed cloud variables as the lower edge of the q_c and q_r fields extends upward from the center to the left portion of the cross sections (Figs. 8b and d).

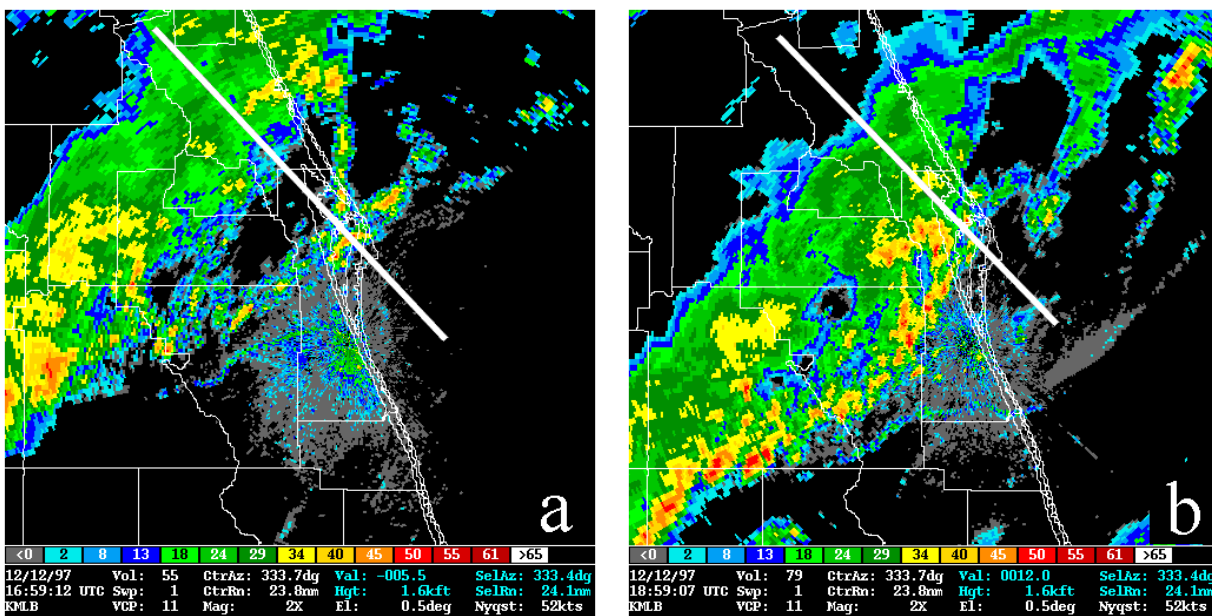


Figure 9. Base reflectivity images from the Melbourne WSR-88D on 12 December 1997 at (a) 1659 UTC and (b) 1859 UTC.

Impact of METAR Cloud Observations

Since satellite data archived by the AMU were available at 15 and 45 minutes past the hour, the warm season cloud analyses are shown at off-hour times. Therefore, no METAR cloud observations are included in the CCS products of Figures 8b and d. Without the influence of cloud information from hourly METAR observations, the cloud analysis cannot analyze low-level q_c below the reflectivity data. Therefore, regions of low cloud cover ($< 1 \text{ km}$) may not be properly analyzed at sufficiently far distances from the WSR-88D site during off-hour times.

In the winter case, features evident in the analyzed cloud cross sections include the presence of multiple horizontal layers of uniform q_c especially below 5 km (Figs. 10b and d). Layers of q_c on the order of $0.1\text{--}0.5 \text{ g kg}^{-1}$ appear at 1 and 4 km on the right side of the cross section in Figure 10b and at 0.25 km on the left side of both cross

sections in Figures 10b and d. In addition, the low-level q_c field for the winter case does not slope upward as in the summer case (Figs. 10b and d). The low-level cloud structure shown for the winter case, especially at levels below 5 km, results from the incorporation of METAR data. The CCS analyzes horizontal layers of q_c in the cross section from METAR observations of multiple cloud layers at different stations within the analysis domain.

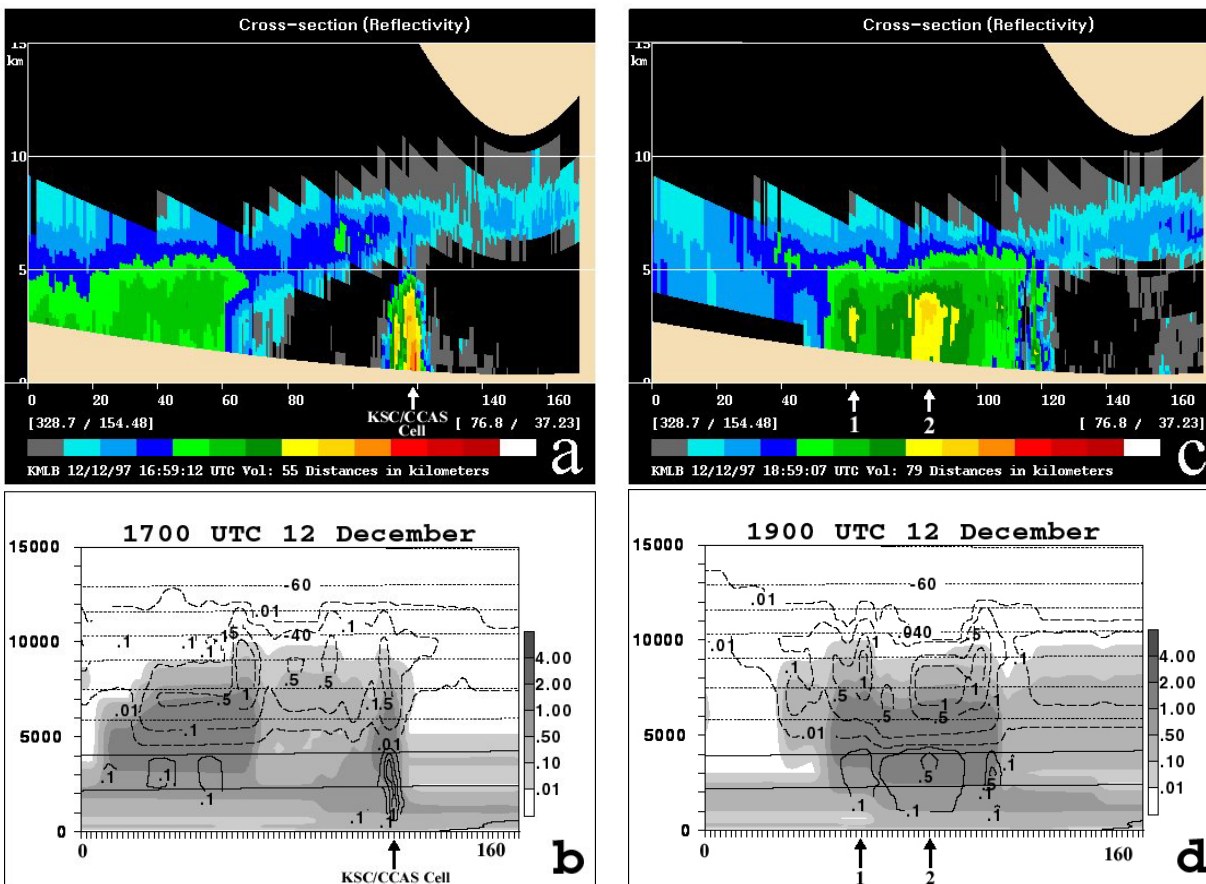


Figure 10. Cross sections of radar reflectivity from the Melbourne, WSR-88D and 2-km ADAS analyses of cloud water mixing ratio (q_c), rain water mixing ratio (q_r), and cloud ice mixing ratio (q_i). All cross sections are taken along the lines shown in Figure 9. Reflectivity cross sections are shown at 1659 UTC and 1859 UTC 12 December 1997 in panels a and c, respectively, while analysis cross sections are shown at 1700 UTC and 1900 12 December 1997 in panels b and d, respectively. The vertical axes range from the surface to 15 km while the horizontal axes range from 0 to 160 km. The q_c fields (g kg^{-1}) are shaded according to the gray scale in panels b and d. The q_r (g kg^{-1}) and q_i (g kg^{-1}) fields are shown by the solid and dashed lines, respectively, in panels b and d. Note that isopleths for q_r (q_i) are given at 0.1, 0.5, and 1.0 g kg^{-1} (0.01, 0.1, 0.5, and 1.0 g kg^{-1}). Horizontal lines in panels b and d denote isotherms every 10 °C with negative temperatures shown by dotted lines. Individual convective cells are marked with arrows.

Summary of CCS Results

Cross sections of cloud variables derived from the CCS of ADAS were compared to radar data for a warm and cool season case study. It was demonstrated that the structure of the cloud analyses resembles the patterns in the reflectivity cross sections. In addition, the insertion of METAR cloud observations for the cool season case was found to generate horizontally uniform cloud layers.

The primary advantage of the CCS is that it integrates METAR, radar, and satellite data to produce a more

complete picture of cloud features over east central Florida. The capability to overlay analyzed cloud variables and other parameters such as temperature can also help forecasters to diagnose cloud properties and possible cloud electrification. In addition, the CCS derives products such as cloud ceiling, cloud tops, fractional cloud coverage, etc. at very high temporal and spatial resolutions. These types of high-resolution products cannot be easily obtained from the individual data sets.

The results from the ADAS cloud analysis shown here represent a portion of the overall task to be presented in the final report. The final report will also focus on the central Florida data deficiency problem, wind analyses from the warm and cool season cases, and results from the data non-incorporation tests.

References

- Albers, S. C., J. A. McGinley, D. A. Birkenheuer, and J. R. Smart, 1996: The local analysis and prediction system (LAPS): Analysis of clouds, precipitation, and temperature. *Wea. Forecasting*, **11**, 273-287.
- Benjamin, S. G., J. M. Brown, K. J. Brundage, D. Devenyi, B. E. Schwartz, T. G. Smirnova, T. L. Smith, L. L. Morone, and G. J. DiMego, 1998: The operational RUC-2. *16th Conf. on Weather Analysis and Forecasting*, Phoenix, AZ, Amer. Meteor. Soc., 249-252.
- Bratseth, A. M., 1986: Statistical interpolation by means of successive corrections. *Tellus*, **38A**, 439-447.
- Brewster, K., 1996: Application of a Bratseth analysis scheme including Doppler radar data. Preprints, *15th Conf. on Weather Analysis and Forecasting*, Norfolk, VA, Amer. Meteor. Soc., 92-95.
- Carr, F. H., J. M. Krause, and K. Brewster, 1996: Application of the Bratseth scheme to high-resolution analyses in inhomogeneous data regimes. Preprints, *15th Conf. on Weather Analysis and Forecasting*, Norfolk, VA, Amer. Meteor. Soc., 231-234.
- Cole, R. E., and W. W. Wilson, 1995: ITWS gridded winds product. Preprints, *6th Conf. on Aviation Weather Systems*, Dallas, TX, Amer. Meteor. Soc., 384-388.
- McGinley, J. A., 1995: Opportunities for high resolution data analysis, prediction, and product dissemination within the local weather office. Preprints, *14th Conf. on Weather Analysis and Forecasting*, Dallas, TX, Amer. Meteor. Soc., 478-485.
- Zhang, J., F. H. Carr, and K. Brewster, 1998: ADAS cloud analysis. Preprints, *12th Conf. on Numerical Weather Prediction*, Phoenix, AZ, Amer. Meteor. Soc., 185-188.

SUBTASK 8 MESO-MODEL EVALUATION (DR. MANOBIANCO)

The Meso-Model Evaluation task was approved by consensus at the AMU Tasking and Prioritization Meeting in June 1998. For this task, the AMU will determine whether a research-quality mesoscale model such as MM5 and/or RAMS (with finer resolution and better physical parameterizations than NCEP's Eta model) is capable of providing added value in forecasting mesoscale signals over Florida during the warm season. The evaluation will compare model forecasts of the sea breeze and convective precipitation following the systematic subjective methodologies used in the AMU's evaluation of NCEP's 29-km Eta model. The task contains two phases. In Phase I, the AMU will provide recommendations as to which models should be included in the evaluation based on factors such as availability of model output and length of data record. In Phase II, the AMU shall perform the evaluation and document the results.

A preliminary assessment of meso-models available for this task indicates that there are currently three possible candidates. These models include MM5 run at the Air Force Weather Agency (AFWA) and Florida Department of Forestry [in cooperation with the Florida State University (FSU) and NWS Tallahassee] and RAMS run at NWS Tampa (TPA). In September 1998, Dr. Manobianco contacted representatives from the AFWA, FSU, and NWS TPA to determine if these agencies have archived at least 50 cases during the 1998 warm season and can provide the digital, gridded model output to the AMU for the evaluation.

2.5 AMU CHIEF'S TECHNICAL ACTIVITIES (DR. MERCERET)

Dr. Merceret continued a study to determine the actual effective vertical resolution of the KSC 50-MHz DRWP. The study also examines the lifetime of mid-tropospheric wind features as a function of their vertical wavelength. Both analyses use spectral techniques applied to the extensively quality controlled DRWP data set developed for the work published in the *Journal of Applied Meteorology*, November 1997 pp. 1567 - 1575. The results will assist in the development of more effective concepts of operation for the profiler and other wind sounding systems including AMPS (which is scheduled to replace radar-tracked Jimspheres before FY 2000). Dr. Merceret completed analysis of the vertical resolution and determined that the DRWP is usually Nyquist limited at 300 m. In a few cases resolution may be as coarse as 475 m, which was the worst case found. The results have been submitted as a note to the *Journal of Oceanic and Atmospheric Technology*. Work on the lifetime of atmospheric features continues.

In collaboration with Dr. Stan Adelfang at NASA/MSFC, Dr. Merceret developed statistical analyses of high temperature extremes at the Shuttle launch complexes (LC-39 A, B) to assist the Shuttle program in deciding whether to modify its high temperature launch commit criterion (LCC). The joint KSC/MSFC effort provided several different statistical approaches to estimating the probability of violating both the current and the proposed LCC. The KSC and MSFC approaches came to the same conclusion – the probability of violating the current LCC is significantly less than 1 percent. The program elected to retain the current LCC.

Dr. Merceret participated in discussions of the effect of the sampling rate of wind measurements at LC-39 on the ground winds LCC for Shuttle. He also supported discussions on a proposed toxic hazard LCC to protect Shuttle visitors on the NASA Causeway. These efforts will continue into the next quarter.

NOTICE

Mention of a copyrighted, trademarked, or proprietary product, service, or document does not constitute endorsement thereof by the author, ENSCO, Inc., the AMU, the National Aeronautics and Space Administration, or the United States Government. Any such mention is solely for the purpose of fully informing the reader of the resources used to conduct the work reported herein.

Acronym List

30 SW	30th Space Wing
30 WS	30th Weather Squadron
45 LG	45th Logistics Group
45 MXS	45th Maintenance Squadron
45 OG	45th Operations Group
45 SW	45th Space Wing
45 WS	45th Weather Squadron
ADAS	ARPS Data Assimilation System
AFB	Air Force Base
AFCCC	Air Force Combat Climatology Center
AFRL	Air Force Research Laboratory
AFMC	Air Force Materiel Command
AFSPC	Air Force Space Command
AFWA	Air Force Weather Agency
AMPS	Automated Meteorological Profiling System
AMU	Applied Meteorology Unit
ARPS	Advanced Regional Prediction System
ATDD	Atmospheric Turbulence and Diffusion Division
CC	Correlation Coefficient
CCAS	Cape Canaveral Air Station
CCS	Complex Cloud Scheme
CSR	Computer Science Raytheon
DAB	Daytona Beach Rawinsonde Station Identification
DNI	Data Non-Incorporation
DRWP	Doppler Radar Wind Profiler
ELV	Expendable Launch Vehicle
ERDAS	Emergency Response Dose Assessment System
FSL	Forecast Systems Laboratory
FSU	Florida State University
FY	Fiscal Year
GOES	Geostationary Orbiting Environmental Satellite
GUI	Graphical User Interface
HTML	Hyper Text Mark-up Link
HYPACT	Hybrid Particle And Concentration Transport
I&M	Improvement and Modernization
IFR	Instrument Flight Rules
IR	Infrared
ITWS	Integrated Terminal Winds System
JSC	Johnson Space Center

Acronym List

KSC	Kennedy Space Center
LAPS	Local Analysis and Prediction System
LC	Launch Complex
LCC	Launch Commit Criteria
LDIS	Local Data Integration System
LIFR	Low Instrument Flight Rules
LMR	Lockheed Martin Raytheon
MCO	Orlando Rawinsonde Station Identification
METAR	Aviation Routine Weather Report
MIDDS	Meteorological Interactive Data Display System
MSFC	Marshall Space Flight Center
MVFR	Marginal Visual Flight Rules
MVP	Model Validation Program
NASA	National Aeronautics and Space Administration
NCAR	National Center for Atmospheric Research
NCDC	National Climatic Data Center
NCEP	National Center for Environment Prediction
NDBC	National Data Buoy Center
NOAA	National Oceanic and Atmospheric Administration
NSSL	National Severe Storms Laboratory
NWS MLB	National Weather Service Melbourne
NWS TPA	National Weather Service Tampa
PC	Personal Computer
PROWESS	Parallelized RAMS Operational Weather Simulation System
PSU	Penn State University
RAMS	Regional Atmospheric Modeling System
REEDM	Rocket Exhaust Effluent Diffusion Model
RSA	Range Standardization and Automation
RUC	Rapid Update Cycle
RWO	Range Weather Operations
SMC	Space and Missile Center
SMG	Spaceflight Meteorology Group
USAF	United States Air Force
UUCP	UNIX to UNIX Copy Protocol
VFR	Visual Flight Rules
VRB	Vero Beach Rawinsonde Station Identification
WFO	Weather Forecast Office
WSR-88D	Weather Surveillance Radar - 88 Doppler
WWW	World Wide Web

Appendix A

AMU Project Schedule 30 September 1998				
AMU Projects	Milestones	Actual / Projected Begin Date	Actual / Projected End Date	Notes/Status
Statistical Short-range Forecast Tools	Determine Predictand(s)	Aug 98	Sep 98	Completed
	Data Collection, Formulation and Method Selection	Sep 98	Feb 99	Continuing On Schedule
	Equation Development	Feb 99	Apr 99	On Schedule
	Tests with Independent Data	Apr 99	May 99	On Schedule
	Tests with Individual Cases	May 99	Jun 99	On Schedule
	Prepare Products, Final Report for Distribution	May 99	Jul 99	On Schedule
AMU MIDDS-X Conversion	Migrate Current Data Display/Archive Procedures to New Platform	Jul 98	Dec 98	On Schedule
MIDDS-X Transition	Technical Expertise/Assistance	Jul 98	Dec 98	On Schedule
LDIS / Central FL Data Deficiency	Identify Mesoscale Data Sources in central Florida	May 97	May 98	Completed
	Identify / Install Prototype Analysis System	Aug 97	Nov 97	Completed
	Case Studies Including Data Non-incorporation	Nov 97	Oct 98	On Schedule
	Final Report	Jul 98	Oct 98	On Schedule
LDIS Extension	Optimize Temporal Continuity of Analyses	Oct 98	Nov 98	On Schedule
	Determine Configuration Changes Required for Simulated Real-time Runs	Nov 98	Feb 99	On Schedule
	Simulate Real-Time Runs	Feb 99	Apr 99	On Schedule
	Determine Deficiencies /Sensitivities of Simulated Real- time Runs	Apr 99	May 99	On Schedule
	Final Report	May 99	Jun 99	On Schedule
Meso-Model Evaluation	Recommend Models for Evaluation	Jul 98	Oct 98	1-month Delay Waiting for MM5 Data Archive
	Perform Evaluation	Jan 99	Apr 99	On Schedule
	Final Report	May 99	Jun 99	On Schedule
Delta Explosion Analysis	Analyze Radar Imagery	Jun 97	Nov 97	Completed
	Run Models/Analyze Results	Jun 97	Jun 98	Completed
	Final Report	Feb 98	Oct 98	Draft report
	Launch site climatology plan	Apr 98	May 98	Completed

AMU Project Schedule				
30 September 1998				
AMU Projects	Milestones	Actual / Projected Begin Date	Actual / Projected End Date	Notes/Status
Model Validation Program	Inventory and Conduct RAMS runs for Sessions I, II, and III	Jul 97	Jul 98	Session I and III completed
	Run HYPACT for all MVP releases	Aug 97	Oct 98	Session I & III completed; Session II PROWESS completed
	Deliver data to NOAA/ATDD	Oct 97	Oct 98	Once Session II HYPACT completed, all data to be submitted.
	Acquire meteorological data for Titan launches	Jul 97	Oct 98	